

# **Title:** Pathologic subtyping of Alzheimer's disease brain tissue reveals disease heterogeneity

**Running Title:** Alzheimer's subtyping reveals heterogeneity

**Authors:** Tiffany G. Lam<sup>1,2 $\delta$</sup> , Sophie K. Ross<sup>1,2 $\delta$</sup> , Benjamin Ciener<sup>1,2</sup>, Harrison Xiao<sup>1,2</sup>, Delaney Flaherty<sup>1,2</sup>, Annie J. Lee<sup>2,3</sup>, Brittany N. Dugger<sup>4</sup>, Hasini Reddy<sup>1,2</sup>, Andrew F. Teich<sup>1,2,3\*</sup>

**Affiliations:**

<sup>1</sup>Department of Pathology and Cell Biology, Columbia University Irving Medical Center, New York, NY 10032, USA

<sup>2</sup>Taub Institute for Research on Alzheimer's Disease and the Aging Brain, Columbia University Irving Medical Center, New York, NY 10032, USA

<sup>3</sup>Department of Neurology, Columbia University Irving Medical Center, New York, NY 10032, USA

<sup>4</sup>Department of Pathology and Laboratory Medicine, School of Medicine, University of California Davis, Sacramento, CA 95817, USA

<sup>$\delta$</sup>  These authors share joint first authorship

\*Corresponding author:

Andrew Teich

Mailing address: 630 West 168<sup>th</sup> Street, PH 15-124, NY NY, 10032

Phone: 212-305-2861

Email: aft25@cumc.columbia.edu

## **Abstract**

In recent years, multiple groups have shown that what is currently thought of as "Alzheimer's Disease" (AD) may be usefully viewed as several related disease subtypes. As these efforts have continued, a related issue is how common co-pathologies and ethnicity intersect with AD subtypes. The goal of this study was to use a dataset constituting 153 pathologic variables recorded on 666 AD brain autopsies to better define how co-pathologies and ethnicity relate to established AD subtypes. Pathologic clustering suggests 8 subtypes within this cohort, and further analysis reveals that the previously described continuum from hippocampal predominant to hippocampal sparing is well represented in our data. Small vessel disease is overall highest in a cluster with a low hippocampal/cortical tau ratio, and across all clusters small vessel disease segregates separately from Lewy body disease. Two AD clusters are identified with extensive Lewy bodies outside amygdala (one with a high hippocampal/cortical tau ratio and one with a low ratio), and we find an inverse relationship between cortical tau and Lewy body pathology across these two clusters. Finally, we find that brains from persons of Hispanic descent have significantly more AD pathology in multiple neuroanatomic areas. We find that Hispanic ethnicity is not uniformly distributed across clusters, and this is particularly pronounced in clusters with significant Lewy body pathology, where Hispanic donors are only found in a cluster with a low hippocampal/cortical tau ratio. In summary, our analysis of recorded pathologic data across two decades of banked brains reveals new relationships in the patterns of AD-related proteinopathy, co-pathology, and ethnicity, and highlights the utility of pathologic subtyping to classify AD pathology.

53 **Keywords:** Alzheimer's disease, pathology, subtype, hippocampal sparing, hippocampal  
54 predominant, Lewy body disease

55

56 **Abbreviated summary:** Multiple groups have shown that what is currently thought of as  
57 "Alzheimer's Disease" (AD) may be usefully viewed as several related disease subtypes. Here,  
58 we utilize two decades of banked cases to demonstrate how co-pathology and ethnicity  
59 intersect with one of the most widely used methods of pathologic subtyping.

60 **Introduction:**

61 Alzheimer's disease (AD) is the leading cause of dementia in the elderly, and is a major cause  
62 of mortality and morbidity [1, 42]. As personalized medicine is pursued as a therapeutic  
63 strategy across multiple diseases [11, 36], an outstanding question in AD research is the extent  
64 to which AD may be usefully thought of as several related disease subtypes. AD pathology  
65 progresses in a stereotyped fashion, and tau and  $\beta$ -amyloid are both now recognized as  
66 spreading along established neuroanatomical stages [8, 49]. Although this pattern is generally  
67 true for the majority of cases, there is emerging evidence of significant variability in these  
68 trends, with tau deposition in particular showing different regional patterns. One of the  
69 foundational papers in this area identified AD subtypes using analysis of tau pathology in  
70 hippocampus and neocortex [35]. This analysis suggested that AD may segregate into three  
71 distinct pathologic subtypes – 1) typical AD, 2) hippocampal sparing (with relatively less tau  
72 pathology in hippocampus than typical AD and relatively more tau in neocortex than typical AD),  
73 and 3) hippocampal predominant (with these relationships reversed). Notably, these pathologic  
74 subtypes align with biological and demographic features, with hippocampal predominant  
75 subjects older than typical AD and more typically female, and hippocampal sparing subjects  
76 younger than typical AD, more typically male, and on average have a faster clinical progression  
77 than typical AD. These subtypes also relate to imaging metrics, as well as differential  
78 responses to therapy [13, 23, 53]. More recent work suggests that rather than bin AD into  
79 hippocampal sparing/predominant subgroups based on arbitrary thresholds of the hippocampal  
80 to cortical tau ratio, it is more useful to view all AD cases on a continuum using this variable  
81 [28].

82  
83 The idea that AD may reflect different disease subtypes has prompted other groups to subtype  
84 AD into new classification groups based on pathologic data [10], transcriptomic data [37], and  
85 multi-omic data [25]. Analogously to the original paper on hippocampal-based AD subtyping,

86 the newer papers that have identified subtype patterning have also identified features that  
87 segregate with subtypes, such as portability of brain multi-omic AD subtypes into multi-omic  
88 blood data in an independent cohort [25], subtype validation in different mouse models as well  
89 as in a replication cohort [37], and prediction of pathologic cluster grouping using MMSE, CSF  
90 data, and ApoE and MAPT genotype [10]. Additional work has suggested alternate pathologic  
91 categorizations that better align with atypical AD clinical variants [40].

92  
93 In addition to varying methods of disease subtyping, a related issue is how common co-  
94 pathologies and ethnicity intersect with AD subtypes. Here, we exploit 20 years of brains  
95 banked at the New York Brain Bank of Columbia University and we apply clustering analysis to  
96 153 pathologic variables recorded on these brains. Using the subset of 666 brains with a  
97 primary pathologic diagnosis of AD, we uncover new relationships between AD pathology and  
98 both Lewy body disease and vascular disease, including an inverse relationship between  
99 cortical tau and Lewy bodies in patients with extensive Lewy body co-pathology. In an effort to  
100 link our analysis to the prior literature in this area, we demonstrate that our clustering aligns with  
101 previously reported hippocampal sparing and hippocampal predominant phenotypes, and we  
102 further demonstrate that Hispanic persons are concentrated in specific AD subtypes and overall  
103 have more severe AD pathology across multiple regions. In summary, this work takes  
104 advantage of a large and well-characterized dataset to better define how co-pathology and  
105 ethnicity interact with AD pathologic subtypes, and builds on prior work documenting disparities  
106 in pathologic disease burden in persons of Hispanic descent.

107

108

109

110

111

112 **Materials and Methods:**

113 *Description of the New York Brain Bank*

114 This study used all available cases with a completed neuropathology report from 2001 to 2022  
115 at the New York Brain Bank (NYBB). The NYBB was founded in 2001 by Dr. Jean Paul  
116 Vonsattel (JPV). The NYBB serves as the pathology core for the Columbia University  
117 Alzheimer's Disease Research Center and has additional prospective autopsy programs for  
118 Parkinson's disease, amyotrophic lateral sclerosis (ALS), multiple sclerosis, Huntington's  
119 disease, and Essential Tremor. For diagnosis, blocks are taken from the following regions  
120 (Brodmann areas (BA) are listed where appropriate): superior frontal cortex (BA 8, 9), posterior  
121 frontal cortex (BA 4), parietal cortex (BA 1, 3, 5, 40), calcarine cortex (BA17, 18, 31),  
122 hippocampal formation at the level of the lateral geniculate body, caudate with putamen and  
123 nucleus accumbens, globus pallidus with putamen and claustrum, amygdala, thalamus with  
124 anterior nucleus, midbrain, upper pons, lower pons, medulla, cerebellum with dentate nucleus,  
125 temporal pole, cingulate gyrus, subthalamic nucleus, and anterior hippocampus with entorhinal  
126 region. These 18 regions form the core of our diagnostic slide set, and pathologic variables from  
127 these blocks were used in this study. A standard slide of luxol fast blue/hematoxylin and eosin is  
128 produced for every block. In addition, immunohistochemistry for phospho-tau (AT8 at 1:200  
129 dilution; Thermo Fisher; Catalog # MN1020),  $\beta$ -amyloid (6E10 at 1:200 dilution; BioLegend;  
130 Catalog # 803003),  $\alpha$ -synuclein (KM51 at 1:40 dilution; Leica; Catalog # NCL-L-ASYN), and  
131 TDP-43 (C-terminal rabbit polyclonal at 1:500 dilution; Proteintech; Catalog # 12892-1-AP) is  
132 performed on blocks where these pathologies are expected to occur [8, 26, 33, 34] (totaling 30  
133 immunostains as our minimal up-front set), in addition to 5 Bielschowsky silver stains on the first  
134 5 blocks listed above (four cortical blocks + hippocampus).

135

136 Note that the above dilutions and antibodies represent the current protocol for brains at our  
137 bank. This study is a retrospective study over the past 20 years, and all of our staining is done  
138 on CLIA certified machines at Columbia University Irving Medical Center (in the Ventana  
139 automated slide stainer, without manual antigen retrieval and visualized using the Ventana  
140 ultraView universal DAB detection kit (Tucson, AZ) as recommended by the manufacturer). We  
141 do not have records of how the antibody concentrations and protocols have changed over the  
142 last 20 years at the immunohistochemistry core, and as such it is not possible to control for this  
143 batch effect over time. A similar point can be made concerning evolving criteria for diagnostic  
144 categories, particularly Alzheimer's disease [2, 34]. Here, we are determining whether historical  
145 data can yield useful insights in AD pathophysiology, with all of the accompanying caveats that  
146 pertain to longitudinal pathologic data (this weakness of our study further discussed in the  
147 Discussion section). In addition, TDP-43 immunostaining was started in our brain bank in 2015  
148 and our standard stain set established in 2018. As a result TDP-43 staining is not done on a  
149 sufficient number of subjects for the below clustering analysis (also a weakness discussed in  
150 the Discussion section).

151

#### 152 *Description of variables used in this study*

153 All of the cases used in this report were signed out between 2001 and 2022 by JPV (although  
154 JPV should be an author on this manuscript due to his extensive efforts, he is retired and not  
155 accepting authorship on manuscripts, see acknowledgements). Cases signed out by JPV had  
156 up to 276 variables recorded to varying degrees, and we exclusively used cases signed out by  
157 JPV for this study due to the fact that this is the large majority of cases at NYBB as of this study,  
158 and also to eliminate interobserver variability in pathologic grading. Of these 276 variables, we  
159 first eliminated variables using thresholding for feature completeness. Only features with at least  
160 60% completeness across all available cases in the brain bank were retained, resulting in 196  
161 pathologic features. Further filtering was applied at the sample level, requiring each case we

162 retained for analysis to have at least 80% of the values across the 196 chosen features (these  
163 thresholding values were chosen after visual inspection of feature abundance curves, with  
164 thresholds chosen where abundance plateaus). After imputing missing data (see below), we  
165 then eliminated redundant features and features that represented summary statistics of other  
166 features, resulting in 153 unique pathologic features for clustering analysis. Additionally,  
167 pediatric cases and cases with unusual/rare diagnoses that did not fall into one of the diagnostic  
168 groups in Figure 1A were eliminated, which resulted in 1433 cases for subsequent clustering  
169 analyses. For the purposes of this study, “primary pathologic diagnosis” is defined by the top  
170 pathology diagnosis listed by JPV in the autopsy report, which he judged to be the diagnosis  
171 with the most severe pathology. Note however that there are frequently additional co-  
172 pathologies in most of our cases, as we are a brain bank for diseases of aging, where  
173 comorbidity is the rule rather than the exception [6, 26, 46]. Indeed, this varying co-pathology is  
174 a major focus of our analysis of AD cases in this paper. Of the 153 variables used for clustering  
175 analysis, 23 involve quantification of  $\beta$ -amyloid in various regions, 38 involve quantification of  
176 phospho-tau (tangles or neurites) in various regions, 36 involve quantification of atrophy or cell  
177 loss, 5 involve quantification of ischemia or vascular disease, 14 involve quantification of Lewy  
178 bodies, and 37 involve other miscellaneous categories (all variables with definitions listed in  
179 Supplemental Data). Pathologic data fell into three general categories; categorical (the  
180 pathologic feature is present/absent), subjectively graded (i.e. pathologic feature exists at low  
181 density, moderate density, or high density, based on experience), and precisely graded (i.e.  
182 each grade corresponding to a specific range of features such as tangles per 100x field).  
183 Examples of subjectively graded categories are displayed in Supplemental Figure 1.

184

### 185 *Clustering of pathologic variables*

186 Missing data imputation was performed using the MICE (Multivariate Imputation by Chained  
187 Equations) method, which is particularly effective for handling missing data in datasets with

188 mixed variable types. MICE generates multiple imputations to account for uncertainty and  
189 provides robust estimates by leveraging relationships between variables. This method was  
190 implemented using the mice package (version 3.16.0) in R [54]. To assess the dissimilarities  
191 between samples, a dissimilarity matrix was generated using the daisy function from the cluster  
192 package in R, applying the Gower metric to effectively handle the mixed dataset containing  
193 numerical and categorical pathological variables.

194  
195 The optimal number of clusters was determined using the gap statistic method, which compares  
196 the total within-cluster variation for different numbers of clusters against their expected values  
197 under a null reference distribution [50]. This was estimated with the clusGap function from the  
198 cluster package in R, utilizing the pam (Partitioning Around Medoids) algorithm as the clustering  
199 method, and analyzing up to a maximum of 20 clusters with 500 bootstrapping iterations. The  
200 optimal number of clusters was identified by examining the graph of gap statistic values, where  
201 the optimal point is where the gap statistic plateaus, indicating that additional clusters do not  
202 significantly improve the clustering structure. This can be defined a number of different ways  
203 [50], and we defined it as the minimum  $\text{Gap}(k) > \text{Gap}(k+1) - 2 \cdot \text{SE}(k+1)$ , and also required that  
204 at least the next three successive  $\text{Gap}(k)$  values also pass this threshold to avoid local changes  
205 in the curve that are not reflective of the overall trend. For the full dataset, this method identified  
206 12 clusters as optimal. When focusing on cases with a first neuropathological diagnosis of  
207 Alzheimer's disease (AD), the same approach revealed that 8 clusters were optimal.

208  
209 PAM was selected for its robustness to outliers and its use of actual data points as cluster  
210 centers (medoids). This characteristic enhances stability in the presence of noise, unlike  
211 centroid-based methods such as K-means, which can be significantly influenced by outliers [3].  
212 By using real data points as medoids, PAM provides more meaningful cluster representatives  
213 compared to the abstract means used in K-means. This is particularly advantageous when



214 dealing with noisy datasets, as K-means and hierarchical clustering methods can be sensitive to  
215 outliers, potentially leading to incorrect cluster assignments.

216

217 *Statistics*

218 Non-parametric tests are used throughout this study (Spearman's correlation coefficients,  
219 Mann-Whitney U test, Kruskal-Wallis ANOVA). Multiple hypothesis correction is done with false  
220 discovery rate, and all p-values have a threshold of 0.05. Age and sex were regressed from  
221 pathologic variables using the lm function in R. Hippocampal to cortical tau ratio was calculated  
222 by averaging the NFT values for CA1 and subiculum and dividing this by the average of the  
223 prefrontal cortex and parietal cortex NFT values for a given case.

224

225

226 **Results:**

227 The overall goal of this study is to use recorded pathologic data on brains in the New York Brain  
228 Bank (NYBB) to better define how co-pathology and ethnicity interact with AD pathologic  
229 subtypes. To do this, we took advantage of the fact that a majority of brains in the NYBB over  
230 the last 20 years have been signed out by a single neuropathologist (Dr. Jean Paul Vonsattel;  
231 although Dr. Vonsattel should be an author on this manuscript due to his extensive efforts, he is  
232 retired and not accepting authorship on manuscripts, see acknowledgements). We only used  
233 brains signed out by this pathologist for this study, which eliminates interobserver variability.

234

235 *Clustering of Pathologic Variables Reproduces Diagnostic Categories and reveals AD*

236 *heterogeneity*

237 We began by assembling all of the available recorded pathologic data on a cohort of 1433  
238 cases regardless of diagnosis, and after thresholding based on data completeness (see  
239 Methods), we used a list of 153 variables for clustering (see Supplemental Data for list of

240 variables). We first asked how useful this data was for recovering known diagnostic categories.  
241 To do this and to take advantage of the heterogeneous nature of the different pathologic feature  
242 categories, we performed Partitioning Around Medoids (PAM) clustering to identify pathologic  
243 clusters within the full dataset of 1433 brains, regardless of primary pathologic diagnosis. This  
244 analysis identified 12 optimal clusters (Figure 1B). When compared to the same datapoints  
245 labeled by primary pathologic diagnosis (Figure 1A), it is clear that several diagnostic categories  
246 correspond well to clusters, while others (such as MSA) are composed of multiple clusters.  
247 Notably, the majority of the AD cases are subdivided into six clusters, suggesting heterogeneity  
248 in this diagnostic group. Although tSNE is not itself a clustering technique, the fact that MSA  
249 cases are viewed separately in the tSNE plot suggests that there is information in our dataset  
250 that can identify these cases, even though the PAM algorithm preferentially splits AD into  
251 subcategories rather than assign a cluster to MSA. This further supports the view that there is  
252 significant heterogeneity in our AD cases that may be further explored.

253  
254 To better define disease heterogeneity within AD we re-clustered all 666 AD cases separately,  
255 yielding 8 AD clusters (Table 1). To identify which pathologic variables varied the most by  
256 cluster, we performed Kruskal-Wallis ANOVA on each variable across all clusters and ranked by  
257 p-value (see Table 2 for select variables; Supplemental Data for full analysis). The top 6  
258 variables by ranked p-value are all Lewy body related pathologies across multiple regions, and  
259 3 are displayed in Table 2 as an example. There is also significant variation of AD-related  
260 pathologic variables (mostly tangles, neuropil threads, and neuritic plaques in various regions),  
261 as well as significant variation in the severity of small vessel disease pathology (i.e. cribriform  
262 change/lacunae in basal ganglia and pons). This analysis suggests that both AD and non-AD  
263 co-pathology distinguishes AD clusters in our analysis.

264

265 In an effort to organize this information further, we began by determining how AD pathology is  
266 varying across cluster. Prior work by Murray et al. have identified three subtypes of AD (typical,  
267 hippocampal sparing, and hippocampal predominant) which have been validated in several  
268 other reports [13, 23, 35, 53], and we began by determining how well these categories organize  
269 the distribution of AD pathology in our clusters. Although originally conceived of as separate  
270 groups, more recent work has demonstrated that the ratio of hippocampal to cortical tau  
271 pathology is more usefully thought of as existing on a continuum [28]. Inspired by this recent  
272 literature, we determined how this ratio varies in our data. To begin, we plotted this ratio by age  
273 across all samples (similarly to [35] we only included cases with Braak NFT stage 4 or higher,  
274 see Methods). This demonstrated a distribution that is similar to prior reports [28], with low  
275 hippocampal/cortical tau ratio cases being the primary population for younger patients, and high  
276 hippocampal/tau ratio cases existing exclusively at higher age points, and an overall positive  
277 significant correlation ( $r = 0.39$ ;  $p\text{-value} = 1.42 \times 10^{-21}$ ; Figure 2). Similarly to prior reports, this  
278 trend also skews female at higher hippocampal/cortical ratios, with 61% of subjects female in  
279 the upper half of the distribution, and 54.6% subjects female in the lower half of the distribution  
280 (a marginally significant difference;  $p\text{-value} = 0.02$  using binomial test,  $p\text{-value} = 0.15$  using Chi-  
281 squared test).

282  
283 Next, we calculated the average hippocampal/cortical tau ratio value for each cluster (shown in  
284 Table 1), and also highlighted each cluster in our graph of ratio vs. age (Figure 2; see  
285 Supplemental Figure 2 for graphs for all 8 clusters). Both average ratios and cluster  
286 distributions reveal trends across samples. Cluster 1 has a ratio similar to the overall group  
287 (Table 1) and its samples are evenly distributed across ratio and age points (Figure 2),  
288 consistent with samples in this cluster being “typical” AD (i.e. without significant cortical or  
289 hippocampal skew). The next three clusters (2, 3, and 4) have lower than average ratio values  
290 (more similar to the hippocampal sparing phenotype), and the next three clusters (5, 6, and 7)

291 have higher than average hippocampal/cortical ratio values (more similar to a hippocampal  
292 predominant phenotype). Cluster 8 is a cluster with low-AD pathologic change overall, and the  
293 ratio is less relevant for these samples, as the majority have a Braak NFT stage lower than 4.  
294 Note that the Murray et al. criteria, while well established, are not the only categorization  
295 scheme suggested for pathologic clustering, and a prominent alternative (Petersen et al.) has  
296 also been proposed based on hierarchical clustering of data [40]. It is more difficult to port  
297 categories based on data clustering across different datasets, and one advantage of  
298 algorithmically defined categories such as the Murray et al. criteria is the ease of applying these  
299 definitions to different datasets. Nevertheless, integration and cross-comparison of pathologic  
300 clustering schema should be the ultimate goal of these investigations (see Discussion).

301

302 *Lewy body pathology and vascular pathology segregate with clusters based on*

303 *hippocampal/cortical tau ratio*

304 Amongst the three low hippocampal/cortical tau ratio clusters (2, 3, and 4), cluster 2 has both  
305 the lowest average ratio and the lowest age of death amongst all clusters (77.56). The next two  
306 low ratio clusters have ratio values lower than average, although less extreme than cluster 2.  
307 Cluster 3 has the highest overall burden of small vessel disease pathology, and is higher than  
308 all other groups (Figure 3). Cluster 4 has extensive Lewy body disease pathology, which we  
309 compare to the other major Lewy body disease group (cluster 7) below.

310

311 Amongst the next three clusters with higher hippocampal/cortical tau ratios (5, 6, and 7), cluster  
312 5 and 6 show demographic features consistent with the previously reported “hippocampal  
313 predominant” phenotype, with older ages of death and a higher % females in cluster 6. Cluster  
314 6 has an even higher hippocampal/cortical ratio than cluster 5, and a higher age of death (the  
315 highest of all clusters, at 89.62). While clusters 5 and 6 are overall very similar, cluster 5 has a  
316 higher average Braak NFT stage and lower hippocampal/cortical ratio, and also significantly

317 more small vessel disease (Figure 3), suggesting that small vessel disease is less severe in  
318 cases at the most extreme end of the hippocampal/cortical tau ratio.

319  
320 The third high hippocampal/cortical ratio group (cluster 7) differs from clusters 5 and 6 in several  
321 aspects. The age of death (79.2) is a full decade younger than clusters 5 and 6, and the  
322 percent female (39%) is the lowest of all clusters, the opposite of the reported sex skew. Lewy  
323 body disease is extensive within this cluster, comparable to the Lewy body disease in cluster 4.  
324 In order to better understand how these two high Lewy body clusters relate to each other and  
325 the rest of the clusters, we examined Lewy body pathology across regions for these two  
326 clusters, and compared to cortical tau pathology across regions (Figure 4). Cases in cluster 4  
327 (the low hippocampal/cortical tau ratio cluster) show extensive cortical tau pathology, while  
328 cluster 7 cases have minimal cortical tau (consistent with these cases having a higher ratio).  
329 Interestingly, Lewy body pathology shows the opposing trend; although present in both, there is  
330 comparatively less in cluster 4 and comparatively more in cluster 7. In an attempt to quantify  
331 this relationship, we analyzed correlation values of Lewy body and NFT/NPT scores across  
332 these cases. When analyzed across all AD cases, there was an expected positive trend,  
333 consistent with prior reports that Lewy body disease and tauopathy often synergize in AD [20,  
334 22]. However, when only considering cases in these two subgroups with high Lewy body  
335 pathology, the opposing trend is seen, with significant negative correlations between extra-  
336 amygdala Lewy body pathology and cortical tau pathology in several areas. Note that Lewy  
337 body pathology across the neuraxis correlates inversely with cortical tau in these cases  
338 presumably because cortical tau strongly differentiates these cases with regards to overall AD  
339 pathologic burden; when expanded to NPT/NFT values across all areas, cortical tau continues  
340 to dominate the significant associations with Lewy body disease (Supplemental Figure 3). Also  
341 note that even in this sub-analysis the amygdala retains a positive trend between Lewy bodies  
342 and overall tau pathology, consistent with the unique role of the amygdala in AD-related Lewy

343 body disease. In light of the above, one possible interpretation of cluster 7 is that cases with the  
344 most  $\alpha$ -synuclein pathology are demographically more similar to PD (see Discussion for  
345 commentary).

346

#### 347 *AD pathology and associated co-pathology interact with Hispanic ethnicity*

348 Finally, 49 of our AD subjects are of Hispanic heritage. Although we do not record country of  
349 origin for all subjects, approximately 70% of Hispanic residents from the Washington Heights  
350 community surrounding our institution are from the Dominican Republic [7], and so it is  
351 reasonable to assume that these demographics are reflected in the Hispanic persons in this  
352 study (also note that race was not included for all of these subjects, so we are only addressing  
353 Hispanic ethnicity here). We asked how all of the above pathologic metrics are affected by  
354 ethnicity from this perspective. The percent of persons who identified as Hispanic significantly  
355 varied across our AD clusters (chi-squared p-value across all groups = 0.003), with cluster 4  
356 showing the highest percentage (for cluster 4 vs. all other cases, binomial test p-value = 0.0007;  
357 chi-squared p-value = 0.00126). It is particularly interesting that the Lewy body-related cluster  
358 4 has the highest percentage of Hispanic cases, given the lack of Hispanic cases in the second  
359 Lewy body-related cluster 7 (see Discussion). In addition, Hispanic heritage predicted a higher  
360 overall burden of disease across multiple modalities, including neuronal loss, neuropil threads,  
361 neuritic plaques, neurofibrillary tangles, and Lewy body pathology (Figure 5). The age of  
362 Hispanic persons with AD was identical to non-Hispanic white persons with AD (mean of 82 in  
363 both cohorts), and there is an insignificant trend towards a higher percent of female subjects in  
364 Hispanic decedents (63.3%) in comparison to non-Hispanic white decedents (56.3%) (p-value =  
365 0.2 by binomial test, p-value = 0.43 by Chi-square test). Consistent with this, regressing for age  
366 and sex has a negligible effect on the significance of these pathologic associations (Figure 5).  
367 In summary, these findings are overall consistent with prior work in this area [45], and suggest

368 that ethnicity is significantly associated with the burden of AD and AD-related pathology (see  
369 Discussion).

370

371 **Discussion:**

372 AD subtyping is still a relatively new area, and the studies to date that use human tissue have  
373 approached the question from a variety of perspectives [10, 25, 37]. An additional limitation for  
374 this field has been that progress necessitates substantial effort and resources from an  
375 established brain bank with decades of well-characterized cases, which unfortunately limits  
376 scientific output in this area. Major questions overlying these investigations include 1) What is  
377 the best way to subtype AD?, and 2) How relevant are these subtypes for understanding AD  
378 pathogenesis and ultimately driving therapeutic strategy?

379

380 Here, we utilize two decades of banked cases at the NYBB to demonstrate how co-pathology  
381 and ethnicity intersect with one of the most widely used methods of pathologic subtyping. In  
382 light of this, it should also be noted that there are a number of alternative ways of subclassifying  
383 AD not evaluated in the current study. Uncommon clinical variants of AD (such as PPA) have  
384 also been linked to different patterns of tau pathology [19, 43, 56], and recent work from  
385 Petersen and colleagues have identified alternate clustering groups that align with these  
386 subtypes better than the hippocampal sparing/hippocampal predominant dichotomy of Murray et  
387 al. [40]. Specifically, Peterson et al. used hierarchical clustering to identify three subtypes with  
388 varying NFT burden (cortical predominant, high overall, and low overall), and demonstrated that  
389 cortical predominant cases have a high proportion of atypical clinical variants. In addition,  
390 Peterson et al. showed that their subgroups align with several clinical and cognitive measures  
391 better than the hippocampal sparing/hippocampal predominant types. As noted earlier, the ratio  
392 of hippocampal/cortical tau may be more useful than the original thresholds for hippocampal  
393 sparing/hippocampal predominant, particularly when looking for significant effects with lower

394 sample sizes, and the hippocampal sparing/hippocampal predominant subtypes have aligned  
395 with additional imaging and clinical data in independent studies [13, 23, 53]. One advantage of  
396 the algorithmic definition of Murray et al. is the ease of analyzing any dataset for these trends,  
397 whereas groupings based on clustered data are often more difficult to port to other datasets,  
398 and we compare our data here to the Murray et al. definitions for both this reason and the  
399 literature supporting the relevance of these findings. Ultimately it will be important to achieve  
400 consensus on the best way to define AD subtypes, which should incorporate not just the Murray  
401 et al. criteria but additional perspectives such as the Peterson et al. categorization.

402  
403 One of the most interesting findings in our data is the relationship of Lewy body pathology to AD  
404 neuropathologic change. LBD is found in 33% to 50% of persons with AD [12, 15, 55], and both  
405 AD and LBD share several common genetic risk factors [4, 12].  $\beta$ -amyloid and tau have both  
406 been shown to interact with  $\alpha$ -synuclein to mutually enhance aggregation [20, 22, 31], and Lewy  
407 bodies localized to the amygdala are so common in AD that a diagnostic category of “amygdala  
408 predominant Lewy body disease” was created to recognize this [32, 33]. Although the amygdala  
409 is an early incubator of Lewy body pathology in AD [32, 33, 41, 52], evidence suggests that  
410 Lewy bodies need to spread outside of this area to have a clinical effect [52]. Indeed, there is  
411 even some evidence that AD patients with amygdala-confined Lewy bodies may have  $\alpha$ -  
412 synuclein aggregates that are less prone to propagation and are therefore less prone to cause  
413 disease [48]. Relatedly, Lewy body disease in the setting of AD appears to have a different  
414 pattern of spread from typical Parkinson’s disease. Specifically, “amygdala only LBD” is almost  
415 exclusively seen in the setting of AD [51, 52], and Lewy bodies are far more likely to spread in  
416 an amygdala-centric fashion in AD, bypassing a more typical progression from brainstem to  
417 cortex [9, 51]. In this context, it is notable that cluster 4 in Figure 4 has more extensive AD  
418 pathology, while Lewy body disease appears to be high in amygdala and limbic structures, and  
419 less prominent in brainstem and cortex, while cluster 7 has less extensive AD pathology but



420 more extensive Lewy body pathology, including brainstem Lewy bodies. Given these pathology  
421 distributions, these two clusters may represent a dichotomy between AD specific amygdala-  
422 driven LBD in cluster 4 vs. more typical PD/LBD in the setting of AD pathology in cluster 7. This  
423 latter cluster is the smaller of the two (33 cases in cluster 7 vs. 76 in cluster 4), and one could  
424 speculate that this smaller cluster simply represents PD/LBD that received a primary pathologic  
425 diagnosis of AD somewhat equivocally over LBD. Indeed, as noted earlier this group is  
426 demographically more similar to PD, with a lower proportion of females and relatively younger  
427 age over the other AD clusters with high hippocampal/cortical tau ratios. Given the differing  
428 relationship between AD and LBD pathology in these clusters, it would be interesting to  
429 investigate whether AD pathology has different effects (in magnitude or degree) in  
430 synergistically driving LBD pathology in these two clusters, and whether they align with  
431 previously identified clinical LBD subtypes [16].

432  
433 Along similar lines, it is interesting that small vessel disease appears more prominent in the low  
434 hippocampal/cortical ratio clusters, with cluster 3 showing the highest level of small vessel  
435 disease. Although vascular pathology and AD pathology are frequently seen in older  
436 individuals, the literature is mixed on whether these two are statistically associated with one  
437 another [14, 24, 27, 30], and a recent meta-analysis suggested that AD pathology and vascular  
438 pathology are uncorrelated [39]. Here, we show that small vessel disease segregates into  
439 specific AD clusters, which suggests that AD pathologic subtyping may help clarify the  
440 relationship between these two pathologies. Vascular disease and Lewy body disease also  
441 segregate differently in our analysis, and this discordance is particularly pronounced in the high  
442 hippocampal/cortical ratio clusters (i.e. comparing cluster 5 vs. 7). Interestingly, the above  
443 mentioned meta-analysis found that Lewy body disease negatively correlated with  
444 atherosclerosis and lacunar infarctions, and these were the only negative associations found  
445 across all age-related pathologies [39]. Although our findings here are broadly consistent with a

446 dissociation between these two co-pathologies, future work should replicate our results or help  
447 clarify a negative association.

448

449 Our work also adds to the growing literature documenting how ethnicity influences the  
450 development of AD pathology [17, 21, 29, 38, 44, 45, 47, 58, 59]. Interestingly, Hispanic  
451 persons are not uniformly distributed across AD subgroups, and are particularly concentrated in  
452 cluster 4 (the high Lewy body disease group with a low hippocampal/cortical tau ratio). This  
453 concentration is particularly striking given the lack of Hispanic persons in the other high Lewy  
454 body group (cluster 7), with a high hippocampal/cortical tau ratio. These findings suggest that  
455 the development of extensive Lewy body co-pathology in Hispanic AD subjects may mostly or  
456 exclusively occur in the setting of high cortical AD pathology, although our sample size is low  
457 and these results need to be replicated. We also found increased burden of several individual  
458 pathologic variables in Hispanic persons. Although some have found evidence of higher tau  
459 deposition in Hispanic persons that survives adjustment for age and sex [45], others have found  
460 higher tau burdens that do not survive adjustment for sex, age of onset, or disease duration  
461 [44]. Hispanic persons with AD have also been shown to have more extensive co-pathology [17,  
462 45, 58, 59], including more small vessel disease [17, 59] (although see [45]), and more Lewy  
463 body disease [58] (although see [44]). We found a higher burden of several pathologic variables  
464 in Hispanic decedents, and in our data these associations survive adjustment for age and sex.  
465 As noted above, higher levels of AD pathology in Hispanic persons are variably dependent on  
466 different demographic factors [44, 45]. Future work should examine how these factors interact  
467 with ethnicity, and why associations with ethnicity variably survive controlling for demographic  
468 factors in different studies. An additional challenge when comparing persons who identify as  
469 Hispanic to persons who do not is potential differences in socioeconomic status, which are  
470 known to independently affect AD progression [57], and are rarely controlled for given the  
471 difficulty of routinely obtaining an objective measure of this information. Indeed, there are many

472 aspects influencing differences in ethnicity and race reported in the literature, including but not  
473 limited to access to care, poverty, education, living conditions, culture, stress, and systemic,  
474 institutional, and individual racism [5, 45, 60, 61]. Finally, in addition to different ways of  
475 measuring pathology, the literature examining the role of Hispanic ethnicity on AD pathologic  
476 change needs to account for the diverse range of backgrounds that identify as Hispanic [18], as  
477 well as chronically low brain bank enrollment of Hispanic patients. Although we do not keep  
478 track of country of origin for all subjects, our local community in Washington Heights is  
479 predominantly of Caribbean Hispanic origin (from the Dominican Republic) [7], and it is  
480 reasonable to assume that the majority of our local Hispanic identifying donors reflect this  
481 background. Given all of these confounding issues, it is notable that increased AD pathology is  
482 still reproducibly found in Hispanic individuals in comparison to non-Hispanic white subjects.  
483 The work presented here adds to this literature, and underscores the importance of continuing  
484 to examine this phenomenon and understand its etiology.

485  
486 Our work has several other limitations. This study is a retrospective study over the past 20  
487 years, and as noted in the Methods, we do not have records of how the antibody concentrations  
488 and protocols have changed over the last 20 years at the immunohistochemistry core where our  
489 staining is performed. As such it is not possible to control for this batch effect over time. A  
490 similar point can be made concerning evolving criteria for diagnostic categories, particularly  
491 Alzheimer's disease, which was updated in 2012 [2, 34]. Here, we are determining whether  
492 historical data can yield useful insights in AD pathophysiology, with all of the accompanying  
493 caveats that pertain to longitudinal pathologic data. Despite these caveats, the fact that we are  
494 able to reproduce aspects of previously defined pathologic subtypes is partial validation that our  
495 approach is scientifically useful. Finally, TDP-43 immunohistochemistry was started at the  
496 NYBB in 2015 and our final stain set with AD cases was established in 2018, and as such we do  
497 not have data on a high enough number of subjects in this study to allow for inclusion of TDP-43

498 data in our clustering. Future work will focus on staining historical cases from our cohort for  
499 TDP-43, which will allow for more complete analysis of the role of TDP-43 proteinopathy in  
500 defining disease subtypes in AD and other neurodegenerative diseases.

501  
502 In conclusion, we have presented clustering data from cases from our brain bank that identifies  
503 and builds on previously established AD subtypes. We have shown that AD clustering identifies  
504 trends in the coincidence of comorbid disease, and have provided additional evidence for the  
505 role of ethnicity in the development of AD pathology. Future work should further integrate  
506 clustering schema across the field and work towards a consensus definition of optimal AD  
507 subtypes.

508  
509  
510 **Supplemental Data:** This contains a list of all pathologic variables and definitions; also shown  
511 are results from a Kruskal-Wallis ANOVA test for all variables across AD groups (select  
512 variables from this list are displayed in Table 2).

513

514

515

516

517

## 518 **Abbreviations**

519

### 520 Pathology

521 NP – neuritic plaque

522 NL – neuronal loss

523 NFT – neurofibrillary tangle

524 NPT – neuropil threads  
525 LB – Lewy body  
526 IP – immature plaque (diffuse plaques)  
527 GCI – glial cytoplasmic inclusion  
528 BN – ballon neuron  
529 Marinesco\_B – Marinesco body  
530  
531 Regions  
532 SNc – Substantia nigra pars compacta  
533 CA1-4 – CA1-4 region of hippocampus  
534 OTG – occipitotemporal gyrus  
535 PHG – parahippocampal gyrus  
536 SI – substantia innominata  
537 TempPole – temporal pole  
538 SNr – Substantia nigra pars reticulata  
539 RN – red nucleus  
540 GPe – external globus pallidus  
541 GPi – internal globus pallidus  
542 CN – caudate nucleus  
543 STN – sub-thalamic nucleus  
544 WM – white matter  
545 HF – hippocampal formation  
546  
547

548 **Ethics approval:** This work uses deidentified pathologic variables and demographic data from  
549 autopsy subjects, and has been determined to be not human subject research by the Columbia  
550 University IRB.

551  
552 **Data availability:** The datasets analyzed during this study are available from the corresponding  
553 author on reasonable request.

554  
555 **Competing Interests:** The authors declare no conflicts of interest

556  
557 **Funding:** This work is supported by NIH grants R01AG072474, P30AG066462, and  
558 R01AG062517.

559  
560 **Acknowledgements:** This work would not have been possible without the meticulous work of  
561 Dr. Jean Paul Vonsattel over a 20 year period. Dr. Vonsattel not only founded the New York  
562 Brain Bank, but generated all of the pathologic data used in this manuscript. As such, he should  
563 be an author, if not a co-senior author, on this manuscript, but he is currently retired and not  
564 accepting authorship on any manuscripts. At minimum, we would like to thank him for his work  
565 that made this manuscript possible, as well as his mentorship to all of the members of the New  
566 York Brain Bank. We dedicate this manuscript to him and his legacy at Columbia University.

567

568

569

## 570 **References**

571

572 1 (2023) 2023 Alzheimer's disease facts and figures. *Alzheimers Dement* 19: 1598-1695  
573 Doi 10.1002/alz.13016

- 574 2 (1997) Consensus recommendations for the postmortem diagnosis of Alzheimer's  
575 disease. The National Institute on Aging, and Reagan Institute Working Group on  
576 Diagnostic Criteria for the Neuropathological Assessment of Alzheimer's Disease.  
577 *Neurobiol Aging* 18: S1-2
- 578 3 (1990) Partitioning Around Medoids (Program PAM). *Finding Groups in Data*, City, pp  
579 68-125
- 580 4 Aarsland D, Creese B, Politis M, Chaudhuri KR, Ffytche DH, Weintraub D, Ballard C  
581 (2017) Cognitive decline in Parkinson disease. *Nature reviews Neurology* 13: 217-231  
582 Doi 10.1038/nrneurol.2017.27
- 583 5 Bailey ZD, Krieger N, Agenor M, Graves J, Linos N, Bassett MT (2017) Structural racism  
584 and health inequities in the USA: evidence and interventions. *Lancet* 389: 1453-1463  
585 Doi 10.1016/S0140-6736(17)30569-X
- 586 6 Barnes LL, Leurgans S, Aggarwal NT, Shah RC, Arvanitakis Z, James BD, Buchman  
587 AS, Bennett DA, Schneider JA (2015) Mixed pathology is more likely in black than white  
588 decedents with Alzheimer dementia. *Neurology* 85: 528-534 Doi  
589 10.1212/WNL.0000000000001834
- 590 7 Bergad L (2008) Washington Heights/Inwood Demographic, Economic, and Social  
591 Transformations 1990 – 2005 with a Special Focus on the Dominican Population. City  
592 University of New York, City
- 593 8 Braak H, Alafuzoff I, Arzberger T, Kretschmar H, Del Tredici K (2006) Staging of  
594 Alzheimer disease-associated neurofibrillary pathology using paraffin sections and  
595 immunocytochemistry. *Acta Neuropathol* 112: 389-404 Doi 10.1007/s00401-006-0127-z
- 596 9 Braak H, Del Tredici K, Rub U, de Vos RA, Jansen Steur EN, Braak E (2003) Staging of  
597 brain pathology related to sporadic Parkinson's disease. *Neurobiol Aging* 24: 197-211  
598 Doi 10.1016/s0197-4580(02)00065-9
- 599 10 Comblath EJ, Robinson JL, Irwin DJ, Lee EB, Lee VM, Trojanowski JQ, Bassett DS  
600 (2020) Defining and predicting transdiagnostic categories of neurodegenerative disease.  
601 *Nat Biomed Eng* 4: 787-800 Doi 10.1038/s41551-020-0593-y
- 602 11 De Strooper B, Karran E (2024) New precision medicine avenues to the prevention of  
603 Alzheimer's disease from insights into the structure and function of gamma-secretases.  
604 *The EMBO journal* 43: 887-903 Doi 10.1038/s44318-024-00057-w
- 605 12 DeTure MA, Dickson DW (2019) The neuropathological diagnosis of Alzheimer's  
606 disease. *Mol Neurodegener* 14: 32 Doi 10.1186/s13024-019-0333-5
- 607 13 Diaz-Galvan P, Lorenzon G, Mohanty R, Mårtensson G, Cavedo E, Lista S, Vergallo A,  
608 Kantarci K, Hampel H, Dubois B et al (2023) Differential response to donepezil in MRI  
609 subtypes of mild cognitive impairment. *Alzheimer's Research & Therapy* 15: 117 Doi  
610 10.1186/s13195-023-01253-2
- 611 14 Dolan H, Crain B, Troncoso J, Resnick SM, Zonderman AB, O'Brien RJ (2010)  
612 Atherosclerosis, dementia, and Alzheimer disease in the Baltimore Longitudinal Study of  
613 Aging cohort. *Ann Neurol* 68: 231-240 Doi 10.1002/ana.22055
- 614 15 Dugger BN, Adler CH, Shill HA, Caviness J, Jacobson S, Driver-Dunckley E, Beach TG,  
615 Arizona Parkinson's Disease C (2014) Concomitant pathologies among a spectrum of  
616 parkinsonian disorders. *Parkinsonism Relat Disord* 20: 525-529 Doi  
617 10.1016/j.parkreldis.2014.02.012
- 618 16 Dugger BN, Boeve BF, Murray ME, Parisi JE, Fujishiro H, Dickson DW, Ferman TJ  
619 (2012) Rapid eye movement sleep behavior disorder and subtypes in autopsy-confirmed  
620 dementia with Lewy bodies. *Mov Disord* 27: 72-78 Doi 10.1002/mds.24003
- 621 17 Filshtein TJ, Dugger BN, Jin LW, Olichney JM, Farias ST, Carvajal-Carmona L, Lott P,  
622 Mungas D, Reed B, Beckett LA et al (2019) Neuropathological Diagnoses of Demented  
623 Hispanic, Black, and Non-Hispanic White Decedents Seen at an Alzheimer's Disease  
624 Center. *J Alzheimers Dis* 68: 145-158 Doi 10.3233/JAD-180992



- 625 18 Flanagin A, Frey T, Christiansen SL, Committee AMAMoS (2021) Updated Guidance on  
626 the Reporting of Race and Ethnicity in Medical and Science Journals. *JAMA* 326: 621-  
627 627 Doi 10.1001/jama.2021.13304
- 628 19 Giannini LAA, Irwin DJ, McMillan CT, Ash S, Rascovsky K, Wolk DA, Van Deerlin VM,  
629 Lee EB, Trojanowski JQ, Grossman M (2017) Clinical marker for Alzheimer disease  
630 pathology in logopenic primary progressive aphasia. *Neurology* 88: 2276-2284 Doi  
631 10.1212/WNL.0000000000004034
- 632 20 Giasson BI, Forman MS, Higuchi M, Golbe LI, Graves CL, Kotzbauer PT, Trojanowski  
633 JQ, Lee VM (2003) Initiation and synergistic fibrillization of tau and alpha-synuclein.  
634 *Science (New York, NY)* 300: 636-640 Doi 10.1126/science.1082324
- 635 21 Graff-Radford NR, Besser LM, Crook JE, Kukull WA, Dickson DW (2016)  
636 Neuropathologic differences by race from the National Alzheimer's Coordinating Center.  
637 *Alzheimers Dement* 12: 669-677 Doi 10.1016/j.jalz.2016.03.004
- 638 22 Guo JL, Covell DJ, Daniels JP, Iba M, Stieber A, Zhang B, Riddle DM, Kwong LK, Xu Y,  
639 Trojanowski JQ et al (2013) Distinct alpha-synuclein strains differentially promote tau  
640 inclusions in neurons. *Cell* 154: 103-117 Doi 10.1016/j.cell.2013.05.057
- 641 23 Hanyu H, Koyama Y, Horita H, Watanabe S, Sato T, Kanetaka H, Shimizu S, Hirao K  
642 (2023) Longitudinal patterns of Alzheimer's disease subtypes: A follow-up magnetic  
643 resonance imaging and single-photon emission computed tomography study. *Geriatr*  
644 *Gerontol Int* 23: 919-924 Doi 10.1111/ggi.14712
- 645 24 Honig LS, Kukull W, Mayeux R (2005) Atherosclerosis and AD: analysis of data from the  
646 US National Alzheimer's Coordinating Center. *Neurology* 64: 494-500 Doi  
647 10.1212/01.WNL.0000150886.50187.30
- 648 25 Iturria-Medina Y, Adewale Q, Khan AF, Ducharme S, Rosa-Neto P, O'Donnell K, Petyuk  
649 VA, Gauthier S, De Jager PL, Breitner J et al (2022) Unified epigenomic, transcriptomic,  
650 proteomic, and metabolomic taxonomy of Alzheimer's disease progression and  
651 heterogeneity. *Sci Adv* 8: eabo6764 Doi 10.1126/sciadv.abo6764
- 652 26 James BD, Wilson RS, Boyle PA, Trojanowski JQ, Bennett DA, Schneider JA (2016)  
653 TDP-43 stage, mixed pathologies, and clinical Alzheimer's-type dementia. *Brain* 139:  
654 2983-2993 Doi 10.1093/brain/aww224
- 655 27 Kapasi A, Yu L, Petyuk V, Arfanakis K, Bennett DA, Schneider JA (2022) Association of  
656 small vessel disease with tau pathology. *Acta Neuropathol* 143: 349-362 Doi  
657 10.1007/s00401-021-02397-x
- 658 28 Kouri N, Frankenhauser I, Peng Z, Labuzan SA, Boon BDC, Moloney CM, Pottier C,  
659 Wickland DP, Caetano-Anolles K, Corriveau-Lecavalier N et al (2024) Clinicopathologic  
660 Heterogeneity and Glial Activation Patterns in Alzheimer Disease. *JAMA Neurol* 81: 619-  
661 629 Doi 10.1001/jamaneurol.2024.0784
- 662 29 Kurasz AM, De Wit L, Smith GE, Armstrong MJ (2022) Neuropathological and Clinical  
663 Correlates of Lewy Body Disease Survival by Race and Ethnicity in the National  
664 Alzheimer's Coordinating Center. *J Alzheimers Dis* 89: 1339-1349 Doi 10.3233/JAD-  
665 220297
- 666 30 Launer LJ, Petrovitch H, Ross GW, Markesbery W, White LR (2008) AD brain pathology:  
667 vascular origins? Results from the HAAS autopsy study. *Neurobiol Aging* 29: 1587-1590  
668 Doi 10.1016/j.neurobiolaging.2007.03.008
- 669 31 Mandal PK, Pettegrew JW, Masliah E, Hamilton RL, Mandal R (2006) Interaction  
670 between Abeta peptide and alpha synuclein: molecular mechanisms in overlapping  
671 pathology of Alzheimer's and Parkinson's in dementia with Lewy body disease.  
672 *Neurochem Res* 31: 1153-1162 Doi 10.1007/s11064-006-9140-9
- 673 32 McKeith IG, Boeve BF, Dickson DW, Halliday G, Taylor JP, Weintraub D, Aarsland D,  
674 Galvin J, Attems J, Ballard C et al (2017) Diagnosis and management of dementia with



- 675 Lewy bodies: Fourth consensus report of the DLB Consortium. *Neurology* 89: 88-100  
676 Doi 10.1212/WNL.0000000000004058
- 677 33 McKeith IG, Dickson DW, Lowe J, Emre M, O'Brien JT, Feldman H, Cummings J, Duda  
678 JE, Lippa C, Perry EK et al (2005) Diagnosis and management of dementia with Lewy  
679 bodies: third report of the DLB Consortium. *Neurology* 65: 1863-1872 Doi  
680 10.1212/01.wnl.0000187889.17253.b1
- 681 34 Montine TJ, Phelps CH, Beach TG, Bigio EH, Cairns NJ, Dickson DW, Duyckaerts C,  
682 Frosch MP, Masliah E, Mirra S et al (2012) National Institute on Aging-Alzheimer's  
683 Association guidelines for the neuropathologic assessment of Alzheimer's disease: a  
684 practical approach. *Acta Neuropathol* 123: 1-11 Doi 10.1007/s00401-011-0910-3
- 685 35 Murray ME, Graff-Radford NR, Ross OA, Petersen RC, Duara R, Dickson DW (2011)  
686 Neuropathologically defined subtypes of Alzheimer's disease with distinct clinical  
687 characteristics: a retrospective study. *Lancet Neurol* 10: 785-796 Doi 10.1016/S1474-  
688 4422(11)70156-9
- 689 36 Narasimhan S, Holtzman DM, Apostolova LG, Cruchaga C, Masters CL, Hardy J,  
690 Villemagne VL, Bell J, Cho M, Hampel H (2024) Apolipoprotein E in Alzheimer's disease  
691 trajectories and the next-generation clinical care pathway. *Nature neuroscience* 27:  
692 1236-1252 Doi 10.1038/s41593-024-01669-5
- 693 37 Neff RA, Wang M, Vatanserver S, Guo L, Ming C, Wang Q, Wang E, Horgusluoglu-  
694 Moloch E, Song WM, Li A et al (2021) Molecular subtyping of Alzheimer's disease using  
695 RNA sequencing data reveals novel mechanisms and targets. *Sci Adv* 7: Doi  
696 10.1126/sciadv.abb5398
- 697 38 Nguyen ML, Huie EZ, Whitmer RA, George KM, Dugger BN (2022) Neuropathology  
698 Studies of Dementia in US Persons other than Non-Hispanic Whites. *Free Neuropathol*  
699 3: Doi 10.17879/freeneuropathology-2022-3795
- 700 39 Nichols E, Merrick R, Hay SI, Himali D, Himali JJ, Hunter S, Keage HAD, Latimer CS,  
701 Scott MR, Steinmetz J et al (2023) The prevalence, correlation, and co-occurrence of  
702 neuropathology in old age: harmonisation of 12 measures across six community-based  
703 autopsy studies of dementia. *Lancet Healthy Longev* 4: e115-e125 Doi 10.1016/S2666-  
704 7568(23)00019-3
- 705 40 Petersen C, Nolan AL, de Paula Franca Resende E, Miller Z, Ehrenberg AJ, Gorno-  
706 Tempini ML, Rosen HJ, Kramer JH, Spina S, Rabinovici G et al (2019) Alzheimer's  
707 disease clinical variants show distinct regional patterns of neurofibrillary tangle  
708 accumulation. *Acta Neuropathol* 138: 597-612 Doi 10.1007/s00401-019-02036-6
- 709 41 Popescu A, Lippa CF, Lee VM, Trojanowski JQ (2004) Lewy bodies in the amygdala:  
710 increase of alpha-synuclein aggregates in neurodegenerative diseases with tau-based  
711 inclusions. *Arch Neurol* 61: 1915-1919 Doi 10.1001/archneur.61.12.1915
- 712 42 Rizzi L, Rosset I, Roriz-Cruz M (2014) Global epidemiology of dementia: Alzheimer's  
713 and vascular types. *Biomed Res Int* 2014: 908915 Doi 10.1155/2014/908915
- 714 43 Rohrer JD, Rossor MN, Warren JD (2012) Alzheimer's pathology in primary progressive  
715 aphasia. *Neurobiol Aging* 33: 744-752 Doi 10.1016/j.neurobiolaging.2010.05.020
- 716 44 Santos OA, Pedraza O, Lucas JA, Duara R, Greig-Custo MT, Hanna Al-Shaikh FS,  
717 Liesinger AM, Bieniek KF, Hinkle KM, Lesser ER et al (2019) Ethnoracial differences in  
718 Alzheimer's disease from the FLorida Autopsied Multi-Ethnic (FLAME) cohort.  
719 *Alzheimers Dement* 15: 635-643 Doi 10.1016/j.jalz.2018.12.013
- 720 45 Scalco R, Saito N, Beckett L, Nguyen ML, Huie E, Wang HP, Flaherty DA, Honig LS,  
721 DeCarli C, Rissman RA et al (2023) The neuropathological landscape of Hispanic and  
722 non-Hispanic White decedents with Alzheimer disease. *Acta neuropathologica*  
723 *communications* 11: 105 Doi 10.1186/s40478-023-01574-1

- 724 46 Schneider JA, Arvanitakis Z, Bang W, Bennett DA (2007) Mixed brain pathologies  
725 account for most dementia cases in community-dwelling older persons. *Neurology* 69:  
726 2197-2204 Doi 10.1212/01.wnl.0000271090.28148.24
- 727 47 Soria JA, Huisa BN, Edland SD, Litvan I, Peavy GM, Salmon DP, Hansen LA, Galasko  
728 DR, Brewer JB, Gonzalez HMet al (2018) Clinical-Neuropathological Correlations of  
729 Alzheimer's Disease and Related Dementias in Latino Volunteers. *J Alzheimers Dis* 66:  
730 1539-1548 Doi 10.3233/JAD-180789
- 731 48 Sorrentino ZA, Goodwin MS, Riffe CJ, Dhillon JS, Xia Y, Gorion KM, Vijayaraghavan N,  
732 McFarland KN, Golbe LI, Yachnis ATet al (2019) Unique alpha-synuclein pathology  
733 within the amygdala in Lewy body dementia: implications for disease initiation and  
734 progression. *Acta neuropathologica communications* 7: 142 Doi 10.1186/s40478-019-  
735 0787-2
- 736 49 Thal DR, Rub U, Orantes M, Braak H (2002) Phases of A beta-deposition in the human  
737 brain and its relevance for the development of AD. *Neurology* 58: 1791-1800
- 738 50 Tibshirani R, Walther G, Hastie T (2002) Estimating the Number of Clusters in a Data  
739 Set Via the Gap Statistic. *Journal of the Royal Statistical Society Series B: Statistical*  
740 *Methodology* 63: 411-423 Doi 10.1111/1467-9868.00293
- 741 51 Toledo JB, Gopal P, Raible K, Irwin DJ, Brettschneider J, Sedor S, Waits K, Boluda S,  
742 Grossman M, Van Deerlin VMet al (2016) Pathological alpha-synuclein distribution in  
743 subjects with coincident Alzheimer's and Lewy body pathology. *Acta Neuropathol* 131:  
744 393-409 Doi 10.1007/s00401-015-1526-9
- 745 52 Uchikado H, Lin WL, DeLucia MW, Dickson DW (2006) Alzheimer disease with  
746 amygdala Lewy bodies: a distinct form of alpha-synucleinopathy. *J Neuropathol Exp*  
747 *Neurol* 65: 685-697 Doi 10.1097/01.jnen.0000225908.90052.07
- 748 53 Uretsky M, Gibbons LE, Mukherjee S, Trittschuh EH, Fardo DW, Boyle PA, Keene CD,  
749 Saykin AJ, Crane PK, Schneider JAet al (2021) Longitudinal cognitive performance of  
750 Alzheimer's disease neuropathological subtypes. *Alzheimers Dement (N Y)* 7: e12201  
751 Doi 10.1002/trc2.12201
- 752 54 van Buuren S, Groothuis-Oudshoorn K (2011) mice: Multivariate Imputation by Chained  
753 Equations in R. *Journal of Statistical Software* 45: 1 - 67 Doi 10.18637/jss.v045.i03
- 754 55 van der Gaag BL, Deshayes NAC, Breve JJP, Bol J, Jonker AJ, Hoozemans JJM,  
755 Courade JP, van de Berg WDJ (2024) Distinct tau and alpha-synuclein molecular  
756 signatures in Alzheimer's disease with and without Lewy bodies and Parkinson's disease  
757 with dementia. *Acta Neuropathol* 147: 14 Doi 10.1007/s00401-023-02657-y
- 758 56 Vogel JW, Young AL, Oxtoby NP, Smith R, Ossenkopppele R, Strandberg OT, La Joie R,  
759 Aksman LM, Grothe MJ, Iturria-Medina Yet al (2021) Four distinct trajectories of tau  
760 deposition identified in Alzheimer's disease. *Nature medicine* 27: 871-881 Doi  
761 10.1038/s41591-021-01309-6
- 762 57 Wang AY, Hu HY, Ou YN, Wang ZT, Ma YH, Tan L, Yu JT (2023) Socioeconomic Status  
763 and Risks of Cognitive Impairment and Dementia: A Systematic Review and Meta-  
764 Analysis of 39 Prospective Studies. *J Prev Alzheimers Dis* 10: 83-94 Doi  
765 10.14283/jpad.2022.81
- 766 58 Wang HP, Scalco R, Saito N, Beckett L, Nguyen ML, Huie EZ, Honig LS, DeCarli C,  
767 Rissman RA, Teich AFet al (2024) The neuropathological landscape of small vessel  
768 disease and Lewy pathology in a cohort of Hispanic and non-Hispanic White decedents  
769 with Alzheimer disease. *Acta neuropathologica communications* 12: 81 Doi  
770 10.1186/s40478-024-01773-4
- 771 59 Weissberger GH, Gollan TH, Bondi MW, Nation DA, Hansen LA, Galasko D, Salmon DP  
772 (2019) Neuropsychological Deficit Profiles, Vascular Risk Factors, and  
773 Neuropathological Findings in Hispanic Older Adults with Autopsy-Confirmed  
774 Alzheimer's Disease. *J Alzheimers Dis* 67: 291-302 Doi 10.3233/JAD-180351

775 60 Yearby R (2020) Structural Racism and Health Disparities: Reconfiguring the Social  
776 Determinants of Health Framework to Include the Root Cause. J Law Med Ethics 48:  
777 518-526 Doi 10.1177/1073110520958876  
778 61 Yearby R, Clark B, Figueroa JF (2022) Structural Racism In Historical And Modern US  
779 Health Care Policy. Health Aff (Millwood) 41: 187-194 Doi 10.1377/hlthaff.2021.01466  
780

## Figure 1

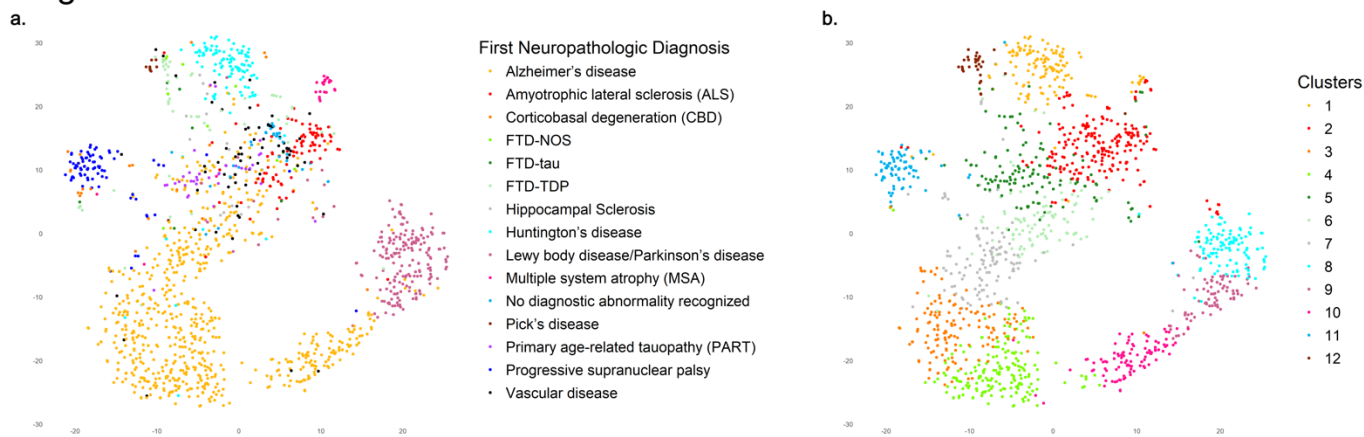
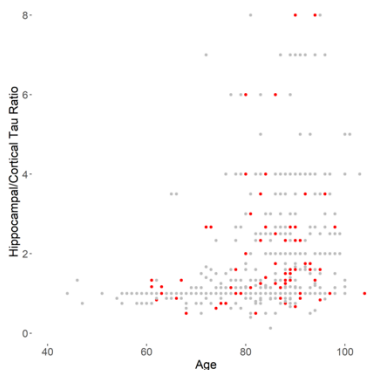


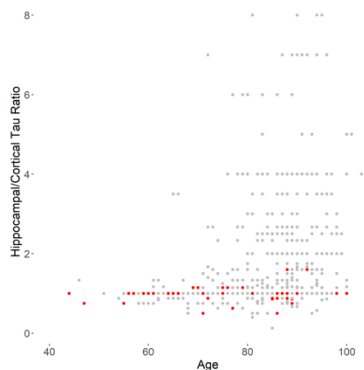
**Figure 1:** Clustering of 1433 cases across the NYBB identifies disease categories. (A) tSNE plot of 153 pathologic variables colored by primary pathologic diagnosis. (B) tSNE plot colored by the 12 identified clusters (see text for details).

## Figure 2

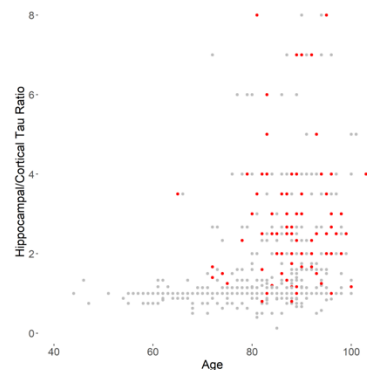
### a. Cluster 1



### b. Cluster 2



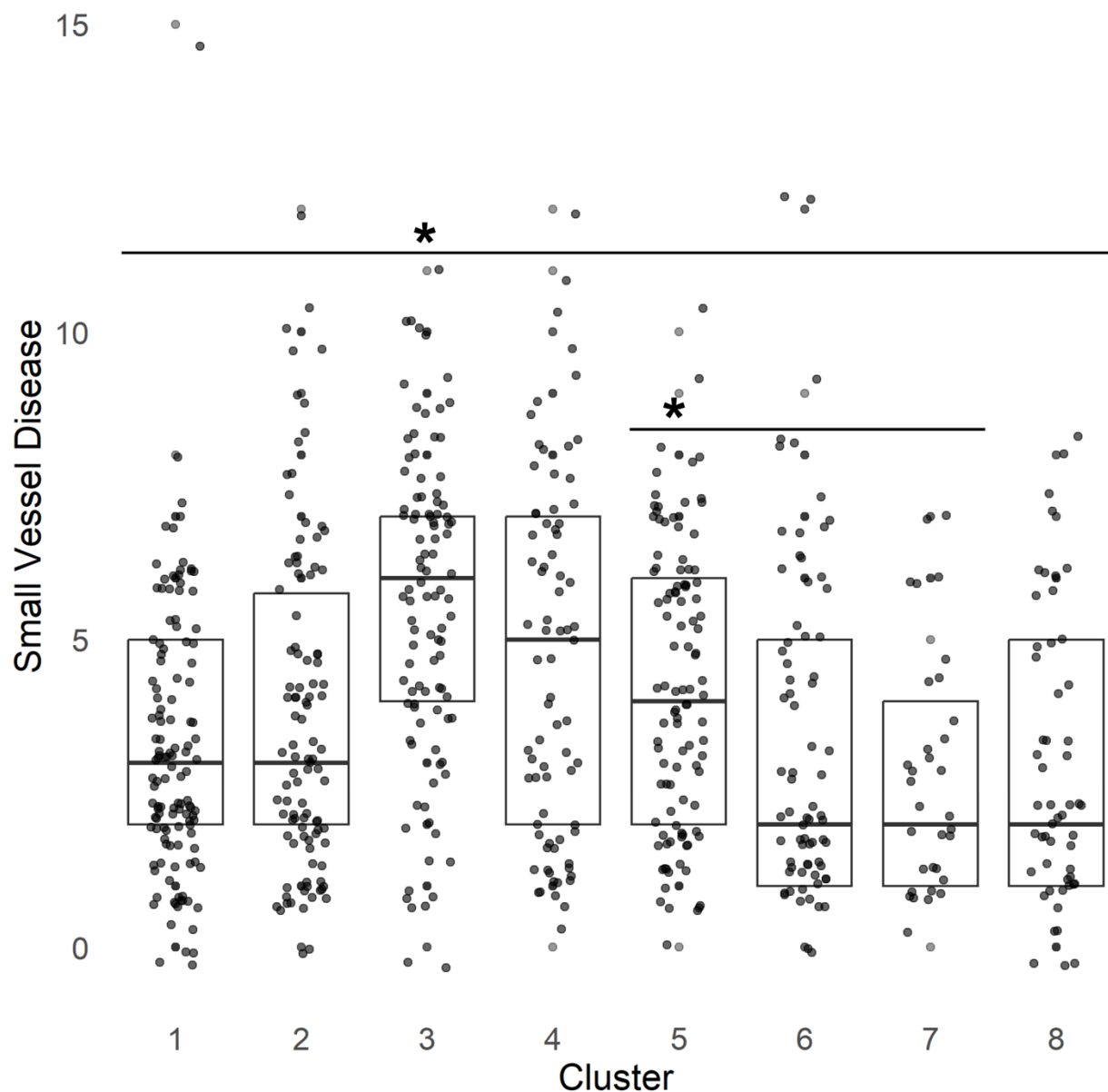
### c. Cluster 5



**Figure 2:** Hippocampal/cortical tau ratios for AD cases with Braak NFT stage of 4 or higher, plotted against age. In (A), (B), and (C), data points from representative clusters are shown in red against all other data points from AD cases. (A) Cluster 1, which is a cluster with an intermediate average hippocampal/cortical tau; (B) Cluster 2, which is a cluster with a lower average hippocampal/cortical tau ratio; (C) Cluster 5, which is a cluster with a higher average hippocampal/cortical tau ratio. Cluster numbers are taken from Table 1; see Supplemental Figure 2 for graphs of all clusters.

## Figure 3

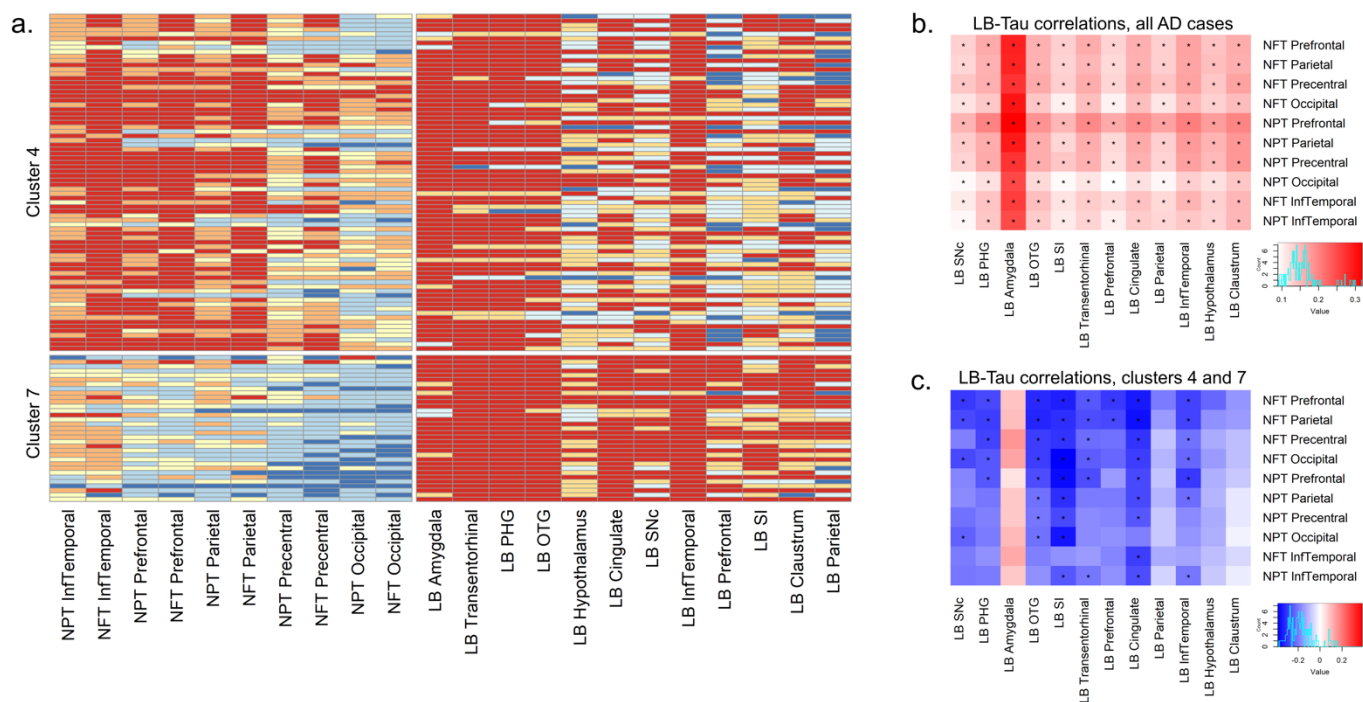
### Small Vessel Disease in AD Clusters



**Figure 3:** Small vessel disease scores (calculated as the sum of scores across four variables; Cribriform/Lacune pathology in pons, caudate, and putamen, as well as overall vascular sclerosis score; see Supplemental Data for definition of pathology variables), are shown for each AD cluster. Cluster 3 shows significantly higher pathology than all other clusters (Mann-Whitney U test p-value < 0.05 vs. cluster 4; less than 0.001 vs. all other clusters). Cluster 5

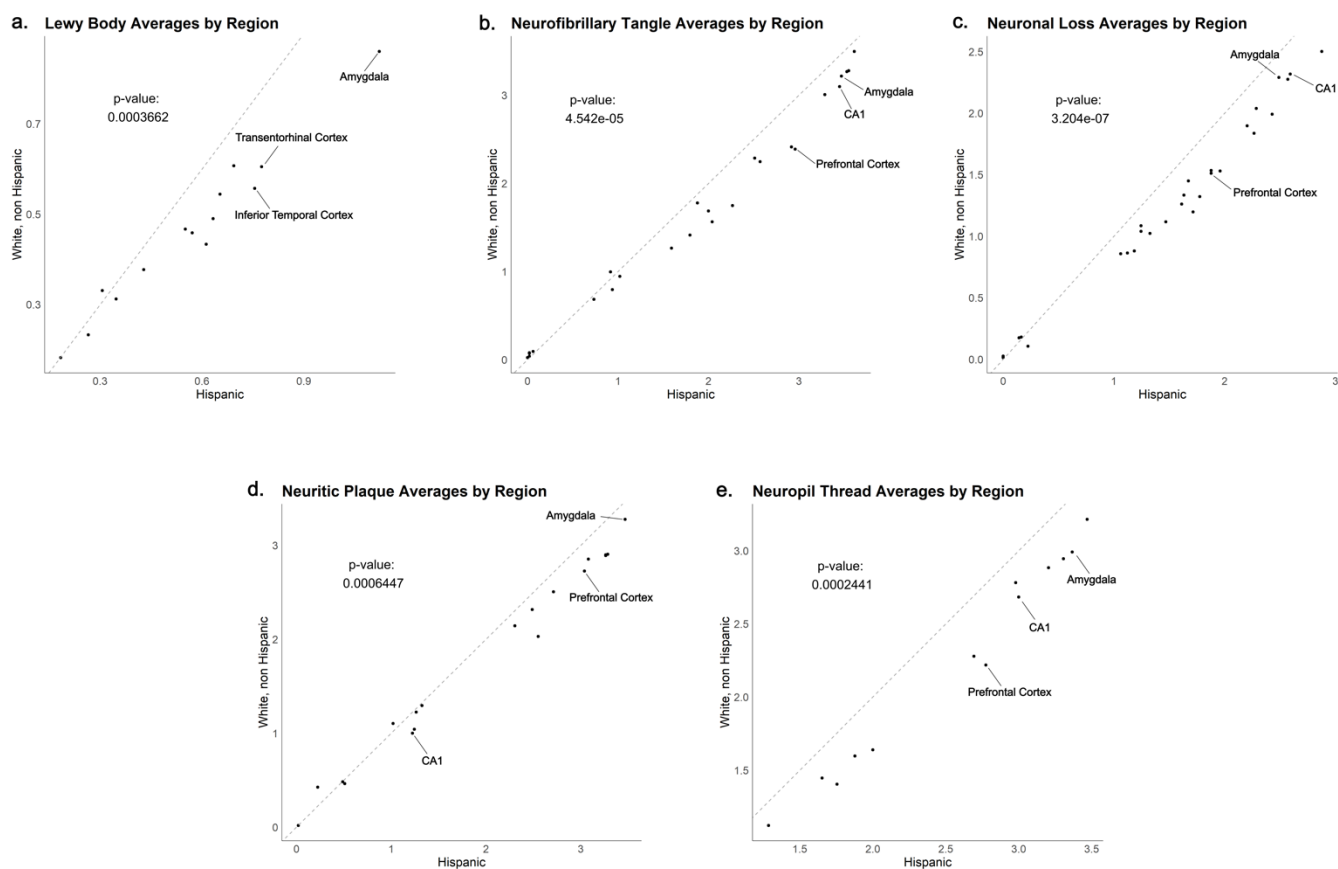
shows more pathology than the other two high hippocampal/cortical tau ratio clusters (clusters 6 and 7; Mann-Whitney U test p-value < 0.01 comparing 5 vs. 6 and 5 vs. 7).

Figure 4



**Figure 4:** Lewy body pathology inversely covaries with tau pathology. (A) Tau pathology and Lewy body pathology heatmaps for AD clusters 4 and 7 (the two high Lewy body disease clusters in Table 1). Cortical tau burden (NFT and NPT) is high in cluster 4 and low in cluster 7. Lewy body pathology in contrast is more extensive in cluster 7 than in cluster 4. While tau and LB pathology co-correlate in the full AD cohort as expected (B), in the subset of patients in clusters 4 and 7 (C), the relationship is largely reversed (starred boxes = FDR adjusted p-value of Spearman's correlation < 0.05). See text for details.

Figure 5



**Figure 5:** Hispanic persons with AD have more extensive pathology than non-Hispanic white persons with AD. For each graph, average values for a given pathology across all measured areas are plotted, with the average of Hispanic persons on the x-axis and the average of non-Hispanic white persons on the y-axis. Representative regions are labeled on each graph. A one-sample Wilcoxon test performed to determine whether the averages significantly deviate from a line with slope = 1 (which would indicate overall equivalent burden between groups) was performed on each graph, with p-value shown. While none of the individual values show a statistical difference between groups, an overall trend of more pathology in Hispanic persons is seen across all shown pathology categories. Note that after controlling for age and sex, all five variables retain significance (p-value < 0.001 for all variables).



Table 1: Demographic and pathologic characteristics of the Eight AD clusters

	1	2	3	4	5	6	7	8	Total
Age	83.52	<b>77.56</b>	<b>80.83</b>	<b>79.82</b>	<b>88.78</b>	<b>89.62</b>	<b>79.18</b>	85.17	83.19
Percent Hispanic	6.4	10.78	7	17.11	3.85	1.37	0	9.43	7.36
Percent Female	56.8	58.82	57	57.89	58.25	63.01	39.39	60.38	57.59
Braak NFT Stage	5.74	5.99	5.88	5.93	5.13	4.42	5.42	3.81	5.41
Braak LB Stage	0.33	0.79	0.5	5.24	0.49	0.48	5.55	0.45	1.3
Hippocampal/Cortical Tau Ratio	1.75	<b>1.00</b>	<b>1.23</b>	<b>1.13</b>	<b>2.86</b>	<b>3.61</b>	<b>2.52</b>	2.00	1.76
Cases Per Cluster	125	102	100	76	104	73	33	53	666

*NFT = Neurofibrillary Tangle, LB = Lewy Body*

*Clusters 2-7 have age and hippocampal/cortical tau ratios that are significantly different when compared to all other cases using Mann-Whitney U test (bolded numbers, p-value less than 0.05).*

Table 2: List of selected pathology variables that significantly vary across AD clusters using a Kruskal-Wallis ANOVA (see Supplementary Data for full list)

Pathology Variable	p-value	p-adj
LB Inferior Temporal	5.21E-112	7.98E-110
LB OTG	5.11E-111	3.91E-109
LB Cingulate	1.04E-106	5.31E-105
NL Parietal	4.34E-101	9.49E-100
NL OTG	1.03E-100	1.98E-99
NFT Parietal	9.11E-100	1.07E-98
NFT Inferior Temporal	1.38E-97	1.24E-96
NFT Prefrontal	2.43E-96	1.95E-95
Cribriform change/lacunae CN	5.75E-14	7.72E-14
Vascular Sclerosis	1.77E-04	2.23E-04

*LB = Lewy Body, OTG = Occipitotemporal Gyrus, NL = Neuronal Loss  
NFT = Neurofibrillary Tangle, CN = Caudate Nucleus*